ChemComm

FEATURE ARTICLE

View Article Online
View Journal | View Issue

Cite this: *Chem. Commun.*, 2016, **52**, 8957

Exploiting redox activity in metal–organic frameworks: concepts, trends and perspectives

D. M. D'Alessandro

Received 27th January 2016,
Accepted 8th March 2016

DOI: 10.1039/c6cc00805d

www.rsc.org/chemcomm

Of the many thousands of new metal–organic frameworks (MOFs) that are now discovered each year, many possess potential redox activity arising from the constituent metal ions and/or organic ligands, or the guest molecules located within their porous structures. Those redox states that can be accessed *via* postsynthetic redox modulation often possess distinct physical properties; if harnessed, these provide a basis for applications including microporous conductors, electrocatalysts, energy storage devices and electrochemical sensors, amongst others. This feature article highlights the latest developments in experimental, theoretical and computational concepts relevant to redox-active MOFs, including new solid state electrochemical and spectroelectrochemical techniques that have great utility in this field. A particular emphasis is on current and emerging trends at the fundamental level which underscore the importance of this promising class of electroactive materials for a wide range of technologically- and industrially-relevant applications.

1. Introduction

The development of redox-active MOFs is a highly sought after goal: at a fundamental level these materials offer unprecedented insights into charge transfer in three-dimensional coordination space; at an applied level, their properties may underpin the next generation of technologically useful devices. Over the past 20 years, MOFs[1,2] have developed at an extraordinary pace owing to the enormous structural and chemical diversity of these highly porous crystalline materials which has spurred myriad potential applications in gas storage, separation and catalysis, amongst others.[3] The potential to exploit the redox-active properties of MOFs is an aspect that has gained attention relatively recently. This can be attributed to the fact that the metal centres (*e.g.*, d^{10} Zn^{II}) and organic linkers (*e.g.*, carboxylates) traditionally used for MOF construction are often redox-inactive.

The redox chemistry of molecular transition metal complexes is an area of significant fundamental interest and importance (*e.g.*, the use of model systems for understanding charge transfer phenomena in nature). For redox-active MOFs, new opportunities are present to explore, for the first time, deeply fundamental aspects of charge transfer within three-dimensional coordination space. In contrast to traditional classes of polymeric and solid state materials such as alloys, metal oxides, mesoporous carbons and zeolites, the molecular nature of MOFs enables an exquisite level of control over their structural, chemical and physical properties at the nanoscale. The presence of cavities and windows due to the crystalline array of nanopores also provides an unprecedented opportunity to exploit host–guest chemistry. The properties of MOFs in their different redox states may be expected to vary significantly due to distinct structural, electronic, magnetic, fluorescent and host–guest properties, amongst others.[4]

The earliest investigations on a redox-active framework material (although not strictly a MOF) are arguably those on Prussian blue, $[Fe^{III}_4\{Fe^{II}(CN)_6\}_3]\cdot xH_2O$, which has been prized industrially for centuries as an ink and dye-stuff. Its "redox isomers" Berlin green (the all-Fe^{III} analogue) and Prussian white (all-Fe^{II} version) can be prepared *de novo* or generated from Prussian blue itself by electrochemical or spectroelectrochemical methods.[5] Despite some ambiguities regarding the exact composition of Fe^{II} and Fe^{III} in various preparations of Prussian blue, the ability to switch between the different redox states has been exploited to modulate the conducting, magnetic, gas adsorption, and optical properties.[5–8]

The historically rich field of metal cyanide frameworks such as Prussian blue offer key insights into the fundamental importance of redox activity in MOFs, and the enormous value of harnessing this property for functional applications. Some important lessons relevant to the broader field of redox-active MOFs are also apparent. These include the need for redox states that are accessible *via* chemical or electrochemical modulation, and the need for stability of these states on the timescale required for measurement. Generating bulk quantities of MOFs in their distinct electronic states requires appropriate chemical oxidants or reductants that do not cause degradation.

School of Chemistry, The University of Sydney, New South Wales, 2006, Australia. E-mail: deanna.dalessandro@sydney.edu.au

Altering the redox state of a framework may have additional structural consequences: (i) it drives the incorporation of a counter-ion for charge balance, and (ii) it may instigate a structural change in the metal- or ligand-based components. In the first case, counter-ion inclusion/expulsion impacts the pore space, and the size and charge of this guest species must be considered in relation to the window aperture and pore size of the framework. Furthermore, despite the addition of a stoichiometric quantity of a chemical oxidant/reductant, the actual extent of the redox change in the framework itself may be limited to surface confined processes, and characterisation must be carefully undertaken. In the second case, MOFs constructed from first-row transition metal centres are notoriously prone to changes in geometry upon redox-state changes, and for this reason, addressing redox activity in such materials may not be possible. In the case of redox-active ligands, radical states (particularly anion radicals) are often sensitive to atmospheric oxygen, making the use of an inert atmosphere for synthesis necessary.

For applications which require a sufficient quantity of MOF, bulk synthesis of the material in a given redox state is required. Meanwhile, *in situ* methods for generating redox states *via* electrochemical means are valuable at the fundamental level for initial measurement of potential redox-accessible states. Recently, *in situ* spectroelectrochemical methods have proven their utility for understanding the fundamental spectroscopic properties of the distinct redox sates.[9]

This article focuses on key experimental, theoretical and computational concepts relevant to redox-active MOFs and highlights current trends in their study at both the fundamental and applied levels. A particular emphasis is how redox activity can be exploited to elucidate charge transfer phenomena, and at the applied level, how the redox-accessible states can be exploited to engender functional properties of technological and industrial importance. Many materials, including ionic MOFs[10,11] for example, may have the potential to exhibit redox activity, but this may not have been probed. The scope is therefore restricted to cases where studies have investigated more than one redox state. Attention is also focused on intrinsic redox activity involving electron or hole movement through the framework backbone,[12] rather than ionic conduction through the pores.[13–15] The discussion here is also restricted to redox transformations that retain the structure of a framework, however, it is interesting to note that amorphous solids derived from ''MOF precursors'' do exhibit highly desirable functional properties.[13] For ease of readability, a list of acronyms for ligands is provided at the end of this article.

2. Fundamental concepts

The highly ordered crystalline structures of MOFs coupled with the potential for systematic tuning of their structural properties offers a unique platform for probing deeply fundamental aspects of charge transfer in multi-dimensional coordination space. Various synthetic methods have been employed to generate redox-active MOFs as single crystals and bulk solids including traditional solvothermal methods and electrosynthesis,[16,17] amongst others.[18,19] Recent developments in fabrication methods for producing highly ordered and oriented thin films[20–24] on surfaces such as conductive substrates has further accelerated the pathway for integrating redox-active MOFs into device architectures.[25–27]

2.1 Engendering redox activity in MOFs

Redox-active MOFs fall in two general classes, where (i) redox-active metals or ligands are present in the as-synthesised framework, or (ii) the redox-active molecules (generally organic species) are introduced postsynthetically into redox-inactive frameworks by covalent bonding or impregnation as guests.[18] In the first case, the origin of the activity arises either from metal centres (which do not alter their geometries upon redox state changes) or ligands (which often possess stable radical states). Although outside the scope of this discussion, even in cases where framework degradation occurs following a redox change, this structural instability has been exploited to produce amorphous materials which have shown promise as electrocatalysts.[28] In cases where the metal centres are magnetically interesting or the ligands possess potential radical states, redox modulation offers a pathway for these materials to be employed as spin probes and in magnetic switching devices.[29] While redox state changes may necessitate the concomitant introduction or expulsion of counterbalancing charges (typically in the form of counter-anions or cations), the remaining pore space can be exploited for functional applications, as discussed in Section 3.

In the second class of redox-active MOFs, the postsynthetic infiltration of redox-active species into redox-inactive frameworks takes advantage of the high affinity of MOFs for non-polar and polar guest molecules. In some cases, redox modulation of the guest induces a change in the electronic properties of the framework, as illustrated by the incorporation of redox-active metallocenes into [VO(bdc)] which induced partial framework reduction.[30] An attractive application for this class of materials is in redox driven release mechanisms.[18] For example, $[Zn_4O(bdc)(btb)_{4/3}]$, otherwise known as UMCM-1, containing alizarin red S or methylene blue as guests exhibited potential driven uptake and release of charge compensating protons upon switching the redox state of the guest.[31,32] Postsynthetic ion metathesis techniques have also proven successful for the introduction of redox-active first-row transition metal ions including Ti^{III}, $V^{II/III}$, $Cr^{II/III}$, Mn^{II} and Fe^{II} into the redox-inactive MOF-5, $[Zn_4O(bdc)]$, scaffold.[33] The synthesis of these metallated analogues could not be achieved using a *de novo* route. This work provided the first evidence for the redox activity of MOF-5 analogues, with the achievement of the stoichiometric single oxidation of Cr^{II}-MOF-5, and the discovery that Fe^{II}-MOF-5 activates NO *via* electron transfer from the Fe centre.[34]

The covalent grafting of redox-active species such as metallocenes into redox-inactive frameworks has been shown to improve the stability of host–guest systems during redox

cycling. A number of frameworks have been targeted in this regard including [Zn(Fcdc)(bpy)],[35] [Zn_4O(bdc-NH_2)(btb)$_{4/3}$] (UMCM-1-NH_2),[36] [Al(OH)(bdc)] (MIL-47(Al)),[37] and the NU-1000 framework consisting of [$Zr_6(\mu_3\text{-}O)_4(\mu_3\text{-}OH)_4(OH)_4(OH_2)_4]^{8+}$ secondary building units linked by 1,3,6,8-tetrakis(*p*-benzoic acid)-pyrene (H_4TBAPy) ligands.[38] Redox hopping between the anchored redox-active groups (*e.g.*, ferrocenyl/ferrocene, Fc^+/Fc) was suggested as the predominant mechanism for charge transport. A particularly interesting observation was the dependence of the permselectivity of ferrocene-functionalised NU-1000 thin-films on the electrolyte concentration: films were permeable to solution cations when the MOF was in the ferrocenium form, but largely impermeable in the ferrocene form.[38] The mechanisms for charge transport within MOF films have been suggested to involve linker[9,39–41] or shuttle-to-shuttle[38] electron/hole redox hopping.[42] The importance of counter-ion diffusion was noted for [Zn(Fcdc)(bpy)],[35] where the redox processes were found to be controlled by the movement of charge compensating counter-anions into the framework upon oxidation of the ferrocene units.

2.2 Redox activity and charge transfer MOFs

A fundamental issue for redox-active MOFs is the question of how charge propagates through the crystal lattice. The mechanisms can be broadly classed as through-bond or through-space and may involve hole or electron transfer. In cases where porosities are low, charge transport is likely to involve surface-confined hopping processes[39] where the redox centres on the surface of MOF particles undergo redox changes while the bulk remains unaffected. This hopping behaviour is also expected for insulating frameworks where the electroactive components are well separated spatially and where effective overlap of frontier orbitals does not exist.

Effective overlap of frontier orbitals and an optimal spatial arrangement of components facilitates charge delocalisation, leading to a conductive framework. An important consideration here is the introduction of counter-ions needed to balance framework charge, which necessarily impedes the porosity.

In addition to the aforementioned strategies for the design of redox-active MOFs, some specific modes of charge transport are also central to the discussion (see Fig. 1).[27,43–45] These modes can involve through-bond charge transfer in the case of highly delocalised systems or through-space transfer by virtue of the close proximity of components. Redox-active moieties are important for facilitating long-range electron transfer, as is already known for one and two-dimensional conductors,[12] however it is important to note that charge delocalisation can take advantage of the organic ligands themselves, with redox-inactive metal centres merely providing "structural support". This π-stacking mediated transfer is exemplified by [Zn_2(TTFTB)(H_2O)$_2$] (Fig. 1a) incorporating benzoate functionalised tetrathiafulvalene (TTF) ligands. Charge transfer occurs along infinite TTF stacks resulting in high electron mobility.[46,47] Indeed, one of the earliest known examples of a coordination polymer exhibiting metallic-like

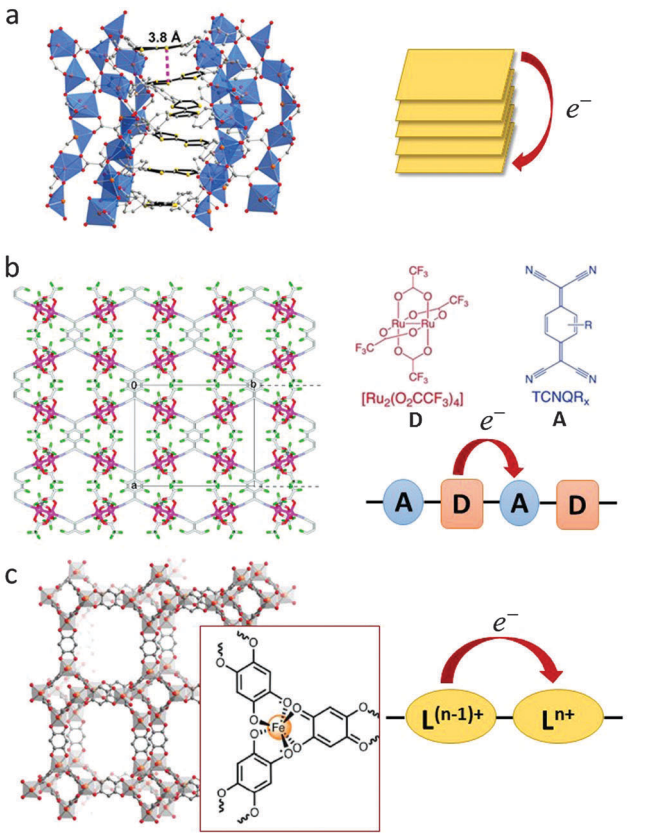

Fig. 1 Examples of strategies for through-bond or through-space charge transfer interactions in MOFs. (a) Side view of a helical TTF stack with a depiction of the shortest intermolecular S–S contact in [Zn_2(TTFTB)(H_2O)$_2$]. Adapted with permission from ref. 46. Copyright 2012 American Chemical Society. (b) Through-bond donor–acceptor charge transfer in [{Ru_2(F_4PhCO)$_4$}$_2$(TCNQ)]. Adapted with permission from ref. 58. Copyright 2010 American Chemical Society. (c) Through-bond mixed valency leading to Intervalence Charge Transfer in [$(NBu_4)_2Fe^{III}_2$(dhbq)$_3$]. The tris-chelating iron centre is highlighted in the insert. L^{n+} and $L^{(N-1)+}$ represent the ligand in its distinct redox states. Adapted with permission from ref. 63. Copyright 2015 American Chemical Society.

conductivity was [Cu(Me_2-DCNQI)$_2$] which featured ligand π–π stacks.[48]

In two-dimensional graphene-like MOFs such as [Ni_3(hitp)$_2$][49] and [Ni_3(bht)$_2$][50] strong π-conjugation supports electron delocalisation through the two-dimensional sheets. Here, there is significant overlap of the metal and ligand frontier orbitals, thus facilitating conductivity.

Two other modes of charge transport can be broadly termed donor–acceptor mechanisms, the origins of which have long and rich historical foundations. In the first case, organic charge transfer (CT) salts constructed purely from organic components have been the source of widespread experimental and theoretical interest for over four decades owing to the exquisite tunability of their electronic structures, and their numerous potential applications in devices such as field effect transistors, photovoltaic cells and light emitting diodes, amongst others.[51–53] The most conductive of these are the so-called "organic metals" including archetypal TTF-TCNQ.[54] Key to CT phenomena in these systems

is the presence of components that can possess stable (neutral, anionic or cationic) radical states. Electronic coupling between the highest occupied molecular orbital (HOMO) of the donor (D) and the lowest unoccupied molecular orbital (LUMO) of the acceptor (A) generates a partial degree of CT (δ) between D and A (also known as the Madelung energy, M), leading to a ground state that is characterised by a partial ionicity.[51,53] The magnitude of δ is dictated by the relative ionisation potential of D (I_D) and electron affinity of A (E_A), where $M(\delta) \approx I_D - E_A$. Three possibilities may arise depending on the magnitude of δ: a neutral or quasi-neutral state ($\delta < 0.5$), a partial CT or mixed-valence state ($0.5 \leq \delta < 1$) state, or a fully ionic state ($\delta = 1$). A plot of the energy of the CT band maximum (ΔE_{CT}) *versus* the potential energy difference between D and A results in the famous Torrance diagram which exhibits a clear boundary between the neutral and ionic states.[55,56] Furthermore, the occurrence of a partial CT state (known as the 'mixed-valence regime') is predicted to generate conductive or metallic-like coordination solids.[57] In addition to these electronic contributions, the structural characteristics of the components (*e.g.*, their degree of planarity) and the arrangement of D and A will also have a critical influence on δ. The degree of CT controls numerous physical properties of CT salts including the lattice energies, bond lengths, optical band gaps and conductivities. Empirical relationships between intrinsic properties of the organic components have also been described using ionicity phase diagrams for the most common CT complexes.[51]

In contrast to organic CT, the understanding of charge transfer interactions in redox-active MOFs is in its infancy. In addition to their increased dimensionality and structural robustness relative to the organic systems, the potential void space in MOFs is highly advantageous for explorations of guest-induced interactions. The first evidence for the applicability of the semiempirical Torrance diagram to coordination solids was reported for through-bond CT in a series of two- and three-dimensional frameworks incorporating carboxylate-bridged paddlewheel-type diruthenium(II,II) units, $[Ru_2^{II,II}(F_4PhCO)_4]$ bridged by $TCNQ^{\bullet -}$ and $DCNQI^{\bullet -}$ radical anions.[58] In these systems, a systematic dependence of the charge transfer energy on the HOMO–LUMO gap of the D (Ru_2) and A (ligand) was reported.[59]

Two recent examples of CT frameworks demonstrate the potential to exploit through-bond or through-space CT mechanisms. In the first case, infiltration of the electron acceptor TCNQ into $[Cu_3(btc)_2]$ (HKUST-1), led to a bridging of the dinuclear copper paddlewheel clusters with the ligands and their partial reduction.[45,60,61] The result was strong through-bond electronic coupling between the units and a concomitant increase in conductivity.[61] By contrast, in the system $[(Zn(DMF))_2(TTFTC)(DPNI)]$, through-space CT interactions have been observed between the electron donor TTF and acceptor DPNI ligands.[62]

A second type of donor–acceptor interaction occurs for a partial CT state ($0.5 \leq \delta < 1$) termed a mixed-valence state, where D and A are the same moiety (either metal- or ligand-based) and are present in different formal oxidation states. A number of three-dimensional frameworks which exhibit mixed-valence states based on the metal centres have been reported.[64] Examples include the pillared bilayer framework consisting of a bismacrocyclic Ni^{II} complex bridged by 1,3,5-benzetricarboxylate ligands, in which intercalation of iodine generates a mixed-valence material containing Ni^{II}/Ni^{III} and I_2/I_3.[65] Certain frameworks have also been prepared directly in mixed-valence form, as exemplified by transition metal cyanide compounds.

For archetypal cyanide-based materials such as Prussian blue, the importance of the mixed-valence phenomenon was first elucidated in the early twentieth century with the realisation that the odd electron was in rapid oscillation between the redox-active Fe^{III} and Fe^{II} centres (rather than being uniquely fixed, one to each ion), giving rise to the absorption of light in the visible or near-infrared (NIR) region of the electromagnetic spectrum.[66] According to the Robin and Day classification scheme,[8] Prussian blue is an example of a ''localised'' Class II system in which the metal ions are weakly-coupled electronically leading to electron hopping.[67] Two additional classes of mixed-valence systems are distinguished on the basis of the extent of charge transfer: Class I systems are characterised by non-interacting centres, and ''delocalised'' Class III systems by strongly-coupled centres. Electronic delocalisation is promoted by mixing between the donor and acceptor wave functions, and in the limit of strong overlap, delocalisation is complete and the metal centres possess identical valences (*i.e.*, the system is conducting).

To date, mixed-valence mechanisms in MOFs have been suggested in a very limited number of cases. A rare example of organic mixed valency was recently reported in the framework $[(NBu_4)_2Fe_2^{III}(dhbq)_3]$ (Fig. 1c).[63] Here, the ligands are present in both their quinone and semiquinone forms ($dhbq^{2-/3-}$), giving rise to an Intervalence Charge Transfer (IVCT) transition. Taking inspiration from the rich literature on mixed valency in dinuclear complexes, conditions for the generation of metal-based mixed-valence MOFs are feasible,[44] as is the possibility of generating mixed valency in MOFs *via* through-space intra-ligand IVCT of the type observed previously in molecular rectangles.[68]

2.3 Spectroscopic methods as a window to redox activity

An important consequence of CT interactions in MOFs is the occurrence of new features in their electronic absorption spectra that are distinct from those of the isolated components themselves. CT interactions of either the through-bond donor–acceptor type,[61] the mixed-valence type,[63] or the through-space donor–acceptor type,[62] are manifested by CT bands in the visible and NIR regions of the electronic absorption spectra. Critically, their analysis provides fundamental information regarding the nature of CT.

Compared with the rare example of the $[(NBu_4)_2Fe_2^{III}(dhbq)_3]$ framework in which an IVCT band was observed,[63] CT in organic mixed-valence systems[69] and dinuclear mixed-valence complexes based on second-row transition metal centres has been studied comprehensively.[66,70–74] The mixed-valence Prussian blue framework has also been the subject of extensive

investigations, and the rate of electron transfer has been calculated from its IVCT band by extracting the electronic coupling and reorganisational energy through application of the Marcus–Hush equation. Some evidence for systematic changes in the IVCT band have also been observed for the ruthenium analogue $K_{1.2}[Ru_{3.6}\{Ru(CN)_6\}_3]$ which exhibited a lower energy band and an increased conductivity, presumably owing to the presence of the second-row transition metals with more diffuse d-orbitals.[75] These spectroscopic signatures of CT may thus provide a window to functional properties of MOFs such as their conductivity. Despite the lack of analyses of CT in MOFs, enormous potential clearly exists to systematically probe these interactions by generating isostructural series of frameworks where the metal centres or organic ligands can be modulated to elucidate structure–function relationships.

2.4 Probing redox activity in MOFs

Solid state electrochemistry (including cyclic and square wave voltammetry) offers the primary tool for interrogating potential redox-accessible states of MOFs, and can provide details on the kinetics and mechanism of charge transfer reactions.[18] Compared with solution state measurements, the electrochemistry of MOFs poses additional challenges due to the more complex processes associated with the various electrode-material and material–electrolyte interfaces, and the intricate ion diffusion processes which are coupled to charge transfer.[76] For example, strong evidence has been found for the dependence of the electrochemical signal of the $Cu^{II/I}$ couple in HKUST-1 on the size of the electrolyte anions/cations (*i.e.*, the current for the $Cu^{II/I}$ couple increased as the size of the cation decreased).[77]

While many reported electrochemical measurements on solid materials have used composites with carbon paste, its use as a conductive supporting matrix precludes accurate analyses of electron transfer parameters. By contrast, relatively simple powder abrasion techniques have proven versatile for adhering solid materials to electrode surfaces and have enabled redox mechanisms to be derived,[78,79] particularly cases that involve charge hopping between redox centres.[35,39]

Where MOFs are insulating and porosities are low, as noted for the ferrocenyl-modified MOF $[Zn_4O(bdc\text{-}NH_2)_{1-x}(bdc\text{-}NHC(O)Fc)_x(btb)_{4/3}]$, surface-confined electron hoping behaviour is expected.[32] Since bulk ion diffusion through the framework was impeded, the peak currents were low relative to the amount of sample, and electron transport was fast leading to a scan rate independence of the peak potentials.

Recently, the application of slow scan cyclic voltammetry (using scan rate of 30 $\mu V\ s^{-1}$ compared with rates typically above 5 $mV\ s^{-1}$) was found to be particularly useful for the reductive insertion of Li^+ (from a $LiBF_4$ electrolyte) into the framework $[(NBu_4)_2Fe_2^{III}(dhbq)_3]$.[63] This method has great future utility for addressing MOFs more broadly, including those assumed to be completely insulating.

Methods to achieve *ex situ* oxidation or reduction involve the use of chemical reagents such as halogens (*e.g.*, Cl_2, Br_2 and I_2), alkali metal salts (*e.g.*, Li or Na napthalenide) or nitrosonium salts amongst others. Matching an appropriate chemical agent to a given redox transformation in a solid is non-trivial, often requiring screening to optimise the conditions. A recent elegant example of the non-innocent nature of redox-active ligands was reported for the framework $[Mn_2(dobdc)]$ (MOF-74) in which addition of a chemical oxidant led to selective oxidation of the $dobdc^{4-}$ ligand to the quinine form $dobdc^{2-}$, whilst maintaining the Mn^{II} oxidation state of the metal centre.[80]

To address some of the issues associated with chemical methods for oxidation/reduction, *in situ* solid state spectroelectrochemical techniques based on UV-vis-NIR, EPR and Raman spectroscopies have recently been developed and successfully applied to MOFs.[9,41,62] In these cases, the spectral response of the material is monitored in real time as a function of the applied potential, with the latter gauged from preliminary electrochemical measurements. Compared with chemical methods for oxidation/reduction, these techniques allow for the relatively rapid identification of the spectral properties of all redox-accessible states of a material, aiding the assignment of the origins of redox processes in electrochemistry based on their spectral signatures. Short lived, or relatively unstable redox-accessible states can thus be identified (*e.g.*, those involving radical anions which are often unstable in the presence of an aerobic environment). Moreover, observation of stable isosbestic points and reversibility of the redox transformations support the retention of structure throughout the process. An important avenue of future work is *in situ* structural determination techniques which provide information on material stability throughout redox transformations.

In the same way that solution state *in situ* spectroelectrochemical methods have proven integral to interrogating fundamental charge transfer properties of soluble molecular species,[81,82] *in situ* solid state UV/vis/NIR, EPR and Raman spectroscopies have now proven their utility for MOFs, particularly in cases where materials degraded during attempts to perform chemical reduction/oxidation.[62,83] Solid state UV/vis/NIR spectroelectrochemistry was first applied to the redox-active framework $[Zn_2(ndc)_2(DPNI)]$, where the spectral signatures of the radical anion and dianion states of the DPNI ligand were observed as a function of the applied potential (Fig. 2).[9] A range of other MOFs have also been interrogated using spectroelectrochemical methods, particularly those incorporating the TTF functionality, an organosulfur moiety that undergoes two reversible one electron oxidations localised on separate rings,[84,85] and NDI, a well-studied electron acceptor.[86] In the case of TTF, a partially oxidised ring has been shown to vastly improve conductivity,[87] while functionalised versions of NDI often display unique electronic, electrochemical and optical properties.[88] The utility of spectroelectrochemical techniques for addressing mechanisms of CT and understanding charge transport mechanisms in thin films of MOFs relevant to electrocatalysis has also recently been demonstrated.[39]

The development of *in situ* solid state EPR spectroelectrochemistry has enabled the interrogation of the charge transfer MOF $[(Zn(DMF))_2(TTFTC)(DPNI)]$, incorporating electron donor TTFTC and acceptor DPNI ligands in a mixed stacking arrangement (Fig. 3).[62] The as-synthesised material exhibited the EPR

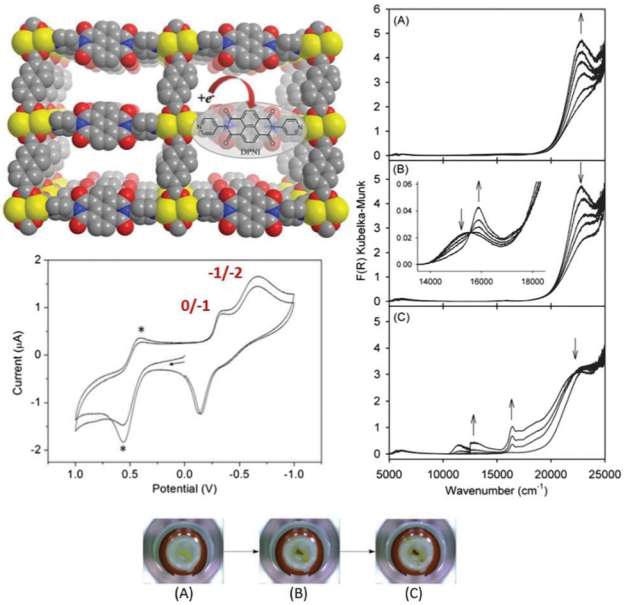

Fig. 2 Solid state electrochemistry and vis/NIR spectroelectrochemistry of $[Zn_2(ndc)_2(DPNI)]$. Cyclic voltammetry reveals two redox waves corresponding to generation of the radical anion and dianion states of the redox-active DPNI ligand. The optical properties of these states can be rapidly accessed using spectroelectrochemistry for generation of the radical anion (A) and dianion (B) states, which are accompanied by marked colour changes as seen in the photographs of the MOF on the transparent working electrode (bottom). Application of a more reducing potential leads to framework degradation (C). Reproduced from ref. 9 with permission from the Royal Society of Chemistry.

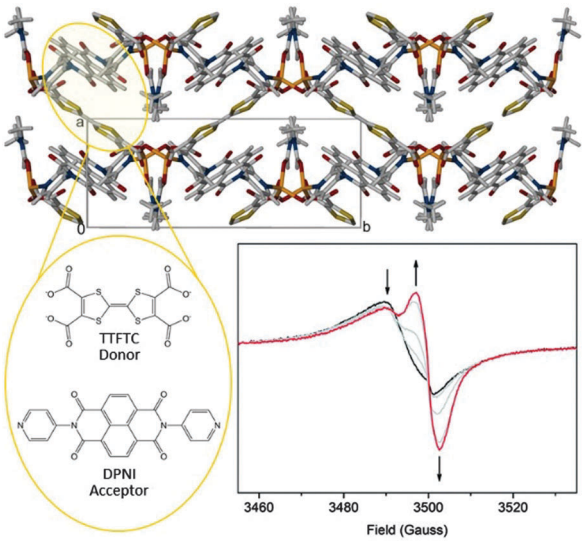

Fig. 3 The charge transfer MOF $[(Zn(DMF))_2(TTFTC)(DPNI)]$ which exhibits through-space CT interactions. Reduction of the MOF switches the CT off. This is consistent with solid state EPR spectroelectrochemistry which revealed evidence for a concomitant decrease in the TTFTC radical cation, and an increase in the DPNI radical anion signal, thus reducing the donor–acceptor interaction. Reproduced from ref. 62 with permission from the Royal Society of Chemistry.

spectrum shown by the black curve in Fig. 3. The splitting of the signal was attributed to two overlapping peaks due to radical species, *i.e.*, a partial CT leads to the coexistence of the $TTFTC^{4-}$ radical cation and DPNI radical anion. At a cathodic potential, the EPR signal due to the $TTFTC^{4-}$ radical cation decreases as the population of DPNI radical anions increases. Coupling the spectral analysis from the EPR spectroelectrochemical reduction with the related UV/vis/NIR measurement proved that partial CT occurred in the as synthesised material. Importantly, this could be reversibly switched on and off by altering the redox state.

In situ solid state fluorescence spectroelectrochemistry has also been applied recently to triarylamine-based frameworks,[89,90] and may prove to be valuable for assessing the function of materials for optoelectronic device applications.

2.5 Computational approaches to redox activity in MOFs

Significant efforts have been devoted to high throughput screening and modelling of the gas adsorption properties of MOFs for their potential applications in gas separations.[91] By comparison, computational studies on the electronic properties of MOFs have been addressed in a relatively limited number of cases.[92]

Modelling redox-active MOFs, particularly those that exhibit significant charge delocalisation, is a challenging task. The extended structures of these materials lead to the introduction of boundary effects for any finite representation. Nevertheless, valuable information has been obtained from density functional theory (DFT) methods by modelling the structures of MOFs as a small number of discrete components in cases where the degree of delocalisation is small. This approach been valuable for modelling the degree of CT in $[(Zn(DMF))_2(TTFTC)(DPNI)]$,[62] where δ was predicted to be 0.6 (*i.e.*, near the mixed-valence regime discussed in Section 2.2) and in the ferrocene functionalised NU-1000 MOF.[93] In the latter case, the Marcus equation was used to describe the rate of intermolecular charge transfer in a chemically relevant fragment from the extended framework crystal structure, and charge transfer was subsequently shown to occur *via* a superexchange mechanism.[38] In addition to modelling the intrinsic charge transfer properties of the MOF, this study also demonstrated the application of computational methods to model MOFs for electrochemical device applications where additional components including the solvent, catalyst and contacts must also be considered.[93]

In the case of $[(Zn(DMF))_2(TTFTC)(DPNI)]$[62] and the ferrocene functionalised NU-1000 MOF,[93] the systems lie at the weak coupling limit and involve localised CT in which charge is likely to hop discretely between sites.[94] While theories pioneered by Hush[95] and Marcus[96,97] may be relevant to charge transfer in the localised limit, they are likely to be inadequate for strongly interacting systems where the classical treatment of nuclear motion is not realistic. Note that localised CT theories have been successfully applied to Prussian blue and Berlin green.[70,98]

Clearly, the development of accurate, low-cost computational methods to describe the electronic properties of MOFs is a highly sought after goal. A key issue is the need for more accurate treatments of dispersion interactions which are important for the description of framework materials and are

also not fully accounted for by traditional functionals based on DFT.[99] New methods must also address the computationally-intensive nature of time-dependent calculations, and deal with approximations for many electron systems which make them prone to inaccuracy.

In an effort to address these challenges, more advanced techniques are currently under development. For example, the DFT-D3 method provides an empirical correction to DFT to account for long-range dispersion interactions, and has already been successfully used to model gas adsorption in MOFs.[100] The Universal Force Field has also recently been extended to deal with transition metal-based MOFs.[101] The density functional theory tight-binding (DFTB) method has enabled high-level electronic structure calculations to be obtained for band gaps.[102,103] An important strategy for the development of improved high-level computational techniques is the need for tandem experimental studies. Measurements on highly ordered systems including single crystals and surface-grafted MOFs (*i.e.*, SURMOFs) are important in this regard.[102]

A further point to note is that particular attention has been focused on characterisation and control of band gaps for applications in electronic and optoelectronic devices.[26] A significant focus has therefore been on computational predictions of the electronic structure of photochromic MOFs where engineering the band gap is of interest for applications in photocatalysis and solar energy harvesting, amongst others.[104]

3. Exploiting redox activity in MOFs: recent developments

Modulating the redox states of MOFs provides access to a range of functional properties that may differ from those of the as synthesised material itself, including magnetism, luminescence and host–guest properties which are relevant to ion diffusion in batteries, and molecular sensing, amongst numerous other applications. Manipulating and controlling the redox state of a material requires application of an external stimulus such as electrical potential, chemical oxidation/reduction, light, pressure or electrical field. Since a number of reviews have detailed the potential applications of ionic and charged MOFs[10] as well as frameworks in which redox activity is central to the function,[18] the emphasis here is on the very latest emerging trends in the field.

3.1 Gas separations and storage

Amongst the most prominent potential applications of MOFs are gas storage and separations processes, for which ligand-based redox activity has predominantly been exploited. In all cases, these studies have involved generation of the different redox states *via ex situ* oxidation or reduction of the materials. In the case of MOFs incorporating redox-active ligands, the result is the creation of a stable radical cation or anion state, and the concomitant incorporation of a counter-ion for charge balance.[105]

Ligand-based redox activity has been exploited in frameworks including $[Zn_2(ndc)_2(DPNI)]$ and $[Zn(ndc)(DBMBI)]$ where the ligands DPNI and DBMBI exhibit stable radical anion states which are generated by reduction with lithium, sodium or potassium napthalenide (XNp where X = Li^+, Na^+ or K^+).[106,107] Gas adsorption studies on the reduced MOFs demonstrated improved uptakes of H_2, CO_2 and CH_4 relative to the neutral parent materials, in addition to increases in the selectivities and isosteric heats of adsorption.[108] The origins of these enhancements were suggested to lie in the catenated nature of the materials: introduction of the alkali metal counter cation upon reduction displaced the interpenetrated networks, thus increasing the pore apertures and surface areas.[109] The uptake was found to be dependent on the amount of chemical reduction, as well as the ionic radius of the alkali metal salt.[110] Beyond an optimum dopant concentration, the adsorbate loading decreased due to pore obstruction by the counterion.

Redox-active MOFs incorporating triarylamine ligands that possess stable radical cation states have also been exploited to fabricate stable metal nanoparticles, and the resulting radical cation impregnated MOFs have demonstrated superior gas adsorption performance relative to their neutral analogues.[111,112] An autoredox reaction between an organic triarylamine species incorporated into a framework led to formation of the radical cation of the triarylamine, whilst metal ions such as Pd^{II}, Ag^{I} and Au^{III} (amongst others) were reduced to the corresponding Pd, Ag or Au metal nanoparticles. Despite a reduction in surface area for the impregnated MOFs, they demonstrated superior H_2 storage performance relative to their neutral counterparts.[75]

While some controversy exists regarding the mechanisms underlying the enhanced gas sorption in reduced or oxidised MOFs, it is typically acknowledged that the included guest (*e.g.*, the counter-cation in the case of framework reduction and the counter-anion in the case of framework oxidation) represent key adsorption sites, and that these may be more important than adsorption onto the framework itself.[113]

A further issue relates to how redox activity might be exploited for industrial-scale gas separations processes (*e.g.*, CO_2 separation from flue gas)[114] given that laboratory experiments performed using *ex situ* methods do not replicate the practical requirements. One possibility is the use of an electrical swing adsorption (ESA) approach for which monolithic carbons have been used previously.[115] This application relies on the Joule effect where the passage of electrical current elicits production of heat which stimulates desorption of adsorbates.[116] Clearly, if these redox-active materials are to be employed in applications such as CO_2 capture, factors such as the switching response times for sorption/desorption will also be critical, as will the energy demands for desorption.

3.2 Electrochromic devices

A common feature of redox state changes in MOFs is the associated colour changes. Commercial applications of electrochromic devices incorporating redox-active systems such as conductive polymers include car mirrors (*e.g.*, Gentex Corporation's antiglare mirrors), electrochromic sunglasses and smart

windows (*e.g.*, adjustable darkening windows in Boeing's 787 Dreamliner).[117]

To date, the most extensively studied framework material for its electrochromic properties is Prussian blue which is readily fabricated as thin films on transparent conductive substrates. Recent work on MOFs has also demonstrated their electrochromic properties,[25,41,118] including the potential to exploit postsynthetic metallation of otherwise redox-inactive materials to introduce redox centres of interest for generating electrochromism.[119] The application of solid state spectroelectrochemistry to MOFs has also revealed their potential polyelectrochromic properties arising from the distinct colours exhibited by several of their redox-accessible states.[62]

Specific requirements for the implementation of electrochromic MOFs in practical applications include favourable contrast ratio, colouration efficiency, cycle life and response time. To address these issues, the framework NU-901, a polymorph of NU-1000, was fabricated as a thin film of 1D free-standing nanorods on transparent FTO conducting glass.[120] The rapid and reversible electrochromic behaviour observed (yellow to deep blue) was attributed to the nanoscale porosity of the MOF. Specifically, the spatial isolation of the redox-active pyrene units in the MOF led to stabilisation of the intensely coloured radical cations (by preventing their dimerisation) upon one electron oxidation.

3.3 Microporous conductors

Typically, MOFs are electronic insulators, or at best, semiconductors due to the nature of the metal centres and bridging ligands which are predominantly carboxylate-based or unsymmetrical (as in the case of CN^-) and do not facilitate strong charge transfer. Of the vast array of crystalline coordination polymers reported to date in the literature, examples of three-dimensional conducting MOFs remain scarce, however, a number of recent studies have made enormous strides in this area.[12,43]

While redox activity alone does not guarantee that a framework material will be intrinsically conducting, effective coupling between redox-active units through overlap of their frontier orbitals is one of the primary means by which conductivity can be achieved. For example, through bond conduction has been suggested to occur through networks of electron-rich heteroatoms such as sulfur in the framework [Mn(dsbdc)].[121] A number of semiconducting 2D frameworks based on triphenylene-derived units have been reported, and their applications have been expanded to include chemiresistive sensing of volatile organic compounds.[122,123]

The opportunity to modulate the redox states of MOFs offers prospects for harnessing switchable conductivity for numerous applications including electrocatalysis and chemiresistive sensing, amongst others.[25,27,43,118] Conducting MOFs have been the subject of excellent recent reviews in the field,[43,45] and the present focus is on cases where the conducting properties have been modulated as a function of redox state. Clearly, for the increasing number of conductive MOFs reported, consideration of potential redox-modulated properties represents a worthwhile pursuit.

Transition metal dithiolene complexes have been employed extensively as redox-active components of MOFs in light of their electronically-delocalised character[50,124–128] which renders them attractive structural motifs for conductive materials. One of the earliest examples of a conductive MOF featuring redox-state dependent conductivity was the dithiolene-based system [Cu{Ni(pdt)$_2$}] which consists of formally Ni^{II} centres coordinated by pdt ligands. Chemical oxidation using I_2 vapour resulted in a 104-fold increase in conductivity which was attributed to electron hopping between the Ni centres, half of which were oxidised to generate a mixed-valence state. In a more recent example, the 2D framework [Ni$_3$(bht)$_2$] exhibited high charge conduction along the 2D sheets which was facilitated by electron delocalisation through the Ni dithiolene moiety.[49,50] The conductivity was also found to be sensitive to the redox-state of the framework.[124]

A number of MOFs exhibit semiconducting behaviour which arises from charge transport *via* organic components, particularly those based on the TTF moiety. Recently, a highly porous Zn^{II} framework, [Zn$_2$(TTFTB)] and a series of isostructural analogues based on Mn^{II}, Co^{II} and Cd^{II}, incorporating a benzoate-functionalised TTF ligand showed both permanent porosity and a high charge mobility that rivalled equivalent organic-based semiconductors.[46] Here, the mechanism of conduction was through the TTFTB stacks.[46,47] The TTFTB ligand has also been integrated into MOFs in combination with various divalent metal ions and neutral coligands.[129] The solid state electrochemical and spectroelectrochemical properties of these materials have demonstrated that two reversible anodic processes corresponding to formation of the radical cation and dication of the TTFTB are accessible. While conductivities for these systems were not reported, the results provided evidence that the properties of the ligand are maintained in the framework.

Redox activity can also be exploited to bring about CT interactions in MOFs which promote long range charge delocalisation and conductivity of the type discussed in Section 2.2. The use of an appropriate D and A pair can induce partial charge transfer which is either through-space[62] or through-bond.[59,61] In the latter case, infiltration of TCNQ into the three-dimensional framework HKUST-1 enhanced the conductivity by seven orders of magnitude.[61] The origin of the enhancement was attributed to postsynthetic coordination of the electron accepting TCNQ moiety to Cu^{II} paddlewheel units forming a conductive pathway that spiralled through voids in framework. A three-state superexchange model was invoked to rationalise the new CT features in the absorption spectra,[45] implying that simple 2-state models may not be sufficient. Semiclassical theories may therefore prove very valuable, as they have for ligand bridged dinuclear complexes which lie in the intermediate Robin and Day[8] Class II–III region for mixed-valence chemistry.[74,130] Subsequent computational work provided structural predictions for MOFs in which similar guest-induced emergent properties may be realised.[131] This post-synthetic approach to introducing the acceptor moiety is particularly valuable for systematically tuning CT interactions (and hence conductivities) of MOFs to obtain structure–function relationships of the type derived for organic CT salts[51] and ruthenium-based MOFs.[59]

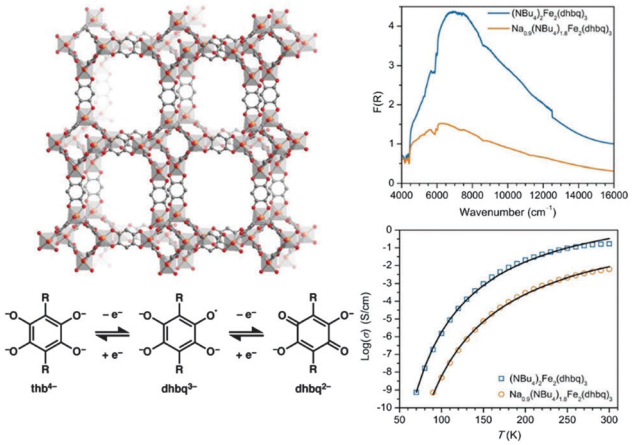

Fig. 4 Schematic of the redox-active framework $[(NBu_4)_2Fe^{II}_2(dhbq)_3]$ (top left). Chemical reduction generates $[(Na)_{0.9}(NBu_4)_{1.8}Fe^{II}_2(dhbq)_3]$ which is accompanied by a decrease in the intensity of the IVCT band (top right) and a decrease in conductivity (bottom right). These observations are consistent with reduction of the mixed-valence $dhbq^{2-/3-}$ ligands (bottom left). Adapted with permission from ref. 63. Copyright 2015 American Chemical Society.

IVCT has also been shown to provide a mechanism for long-range charge delocalisation in the framework $[(NBu_4)_2Fe^{III}_2(dhbq)_3]$ (Fig. 4).[63] Manipulation of the redox state of the MOF *via* chemical reduction dramatically decreased the conductivity by reducing the charge carrier mobility. These conductivity changes were also manifested by a reduction in the intensity of the IVCT band, suggesting a close connection between the spectroscopic band parameters and the bulk conductivity.

In addition to spectroscopic methods that provide an indication of new CT interactions within MOFs, measurements of conductivity must ideally be undertaken on single crystal and crystalline films. These techniques are advantageous compared with conventional pressed pellet measurements on coordination solids in order to minimise grain boundary effects and gain insights into anisotropic conduction.[12]

3.4 Electrocatalysis

While nature has optimised enzymatic processes over the millennia through the use of highly efficient electrocatalytic reactions based on inexpensive, earth-abundant metals such as nickel and iron, the industrial electrocatalysts synthesised today are almost invariably based on expensive and rare platinum-group metals. Spurred by the need for more economically-viable materials based on earth-abundant metals, the development of new classes of electrocatalysts such as MOFs has been gaining momentum owing to their importance in fuel cells for the conversion of chemical energy into electricity[132–134] and renewable energy technologies, amongst other areas.[135]

In contrast to existing materials considered for electrocatalysis including metal oxides, porous metal membranes, nanostructured thin films, metal nanoparticles, conducting polymers and discrete transition metal complexes, MOFs are attractive owing to their high surface areas which provide a large concentration of active sites, and their ability to be used in heterogeneous processes.[42] Progress in this area has been impeded by the instability of some frameworks to redox cycling, and the intrinsic insulating ability of many MOFs which is not conducive to electron migration through the bulk material. Whilst these issues have been addressed in some part through the fabrication of composites,[136] the aforementioned developments in intrinsically conducting MOFs will significantly accelerate progress in this area.

Redox hopping has been shown to provide a mechanism for charge transport within MOFs which have been targeted for a number of electrocatalytic reactions. These processes have largely been focused on key reactions pertinent to artificial photosynthesis including CO_2 reduction and water oxidation. Additional electrocatalytic reactions of interest include the hydrogen evolution reaction (HER), oxygen evolution reaction (OER), oxygen reduction reaction (ORR), alcohol oxidation and nitrite reduction amongst others which have been reviewed recently.[13,18]

A stimulus for the design of MOF-based electrocatalysts has been homogeneous molecular transition metal complexes which are well known for their involvement in particular electrochemical transformations. Inspired by molecular metalloporphyrin electrocatlysts for the reduction of various substrates, a thin film of Fe porphyrin-based $[Zr_6O_4(OH)_4(tccp\text{-}H_2)_3]$ (MOF-525) immobilised on FTO was used to obtain mixture of CO and H_2 from the electroreduction of CO_2.[42] Electrochemical and spectroelectrochemical techniques[9] were also employed to elucidate the mechanism of charge transport in an electrocatalytic cobalt framework based on tccp, where a redox hopping mechanism was proposed. The fabrication of thin MOF films for electrocatalysis were shown to be advantageous.[39,137]

MOFs have also been investigated for water splitting in the context of developing clean energy technologies,[138–140] of which OER and HER are key. Polyoxometalate (POM) based MOFs have received significant attention in the latter case where the extensive electrochemical activity of the POMs in electrocatalytic reactions was exploited.[13] More recently, a MOF film of NU-1000 was used as a support for deposition of a nickel sulfide electrocatalyst.[141] The MOF was shown to improve not only the surface area, but also the proton conductivity of the material.

OER is considered substantially more challenging due to the four-electron nature of this anodic process and the fact that it is performed under alkaline conditions which often promotes framework degradation.[139] Nevertheless, O_2 formation was observed for frameworks such as analogues of $[Zr_6O_4(OH)_4(bpdc)_6]$ (UiO-67), incorporating an Ir-based linker $[Ir^{III}(Cp^*)\text{-}(dcppy)]$ where O_2 was produced. A recent direction in the field is the use of redox-active MOFs as precursors for the preparation of nanoporous carbons and metal oxides.[142]

An important function of the MOF scaffold is the isolation and subsequent stabilisation of potentially highly reactive catalytic metal centres. In some respects, this is analogous to protective protein structures in nature which stabilise haem with high valent iron-oxo species, which are known to activate strong C–H bonds.[143] In this regard, the catalytic conversion of ethane to ethanol was achieved within $[Fe_2(dobdc)]$, a redox-active MOF incorporating a coordinatively unsaturated Fe^{II} site.[143]

Upon activation with N_2O, the Fe^{II} sites were converted to Fe^{III}{hydroxide}, strongly suggesting the presence of an intermediate Fe^{IV}{oxo} species from which C–H bonds could potentially be oxidised. When ethane was passed through the framework, various ethane-derived oxygenates such as ethanol and acetaldehyde were formed.

3.5 Energy storage

One of the earliest electronics applications considered for MOFs was their potential for use as rechargeable intercalation electrode materials and electrochemical double layer capacitors relevant to Li-ion battery technologies for portable electronics and fuel cells. Whilst the process of ion conductivity in MOFs has been extensively reviewed,[13,18,144] ion diffusion through MOF pores and intrinsic electronic conductivity through the framework backbone are interlinked in many materials.

Arguably the first report of a MOF in which the redox activity was exploited in this regard was $[Fe^{III}(OH)_{0.8}F_{0.2}(bdc)]$ (MIL-53(Fe)), which was used as the positive electrode of a Li-ion battery mixed with carbon (Li metal was the negative electrode).[64] Lithium ion insertion generated a mixed-valence framework containing Fe^{III}/Fe^{II} and Li^0/Li^+. Whilst the capacity of the material was poor compared with existing devices, it demonstrated the capability of such materials for repeated discharge/recharge cycles. In this case, the lower than expected capacity was attributed to the lack of permanent porosity which restricted Li-ion motion and prevented complete reduction of the Fe^{III} centres, as well as the existence of a redox-inactive ligand (bdc).

MOFs have also been used for negative electrode materials in the context of lithium storage, where the aforementioned issues of capacity were addressed by exploiting the coexistence of redox activities of the metal and ligand sites.[18] In the redox-active framework [Cu(aqdc)], *in situ* XANES and cyclic voltammetry showed that during the discharge process, both the $Cu_2^{II,II}(acetate)_4$ paddlewheels and anthraquinone groups facilitated the reduction process.[145]

A number of strategies have now been investigated in an effort to surmount issues with the instability of MOF materials over repeat redox cycles, as well as their poor capacitance and low Faradaic efficiencies due to low electrical conductivities and steric hindrance to Li ion insertion.[18] The subject of MOF supercapacitors has been reviewed recently,[144] and whilst outside the scope of this article, the majority of approaches involve the destruction of MOFs *via* pyrolysis, rather than their use as pristine materials. Systems with very high areal capacitance have now been developed by improving the conductivities through doping pristine MOF crystals with graphene[146] or polyaniline chains that have been electrochemically deposited on the MOF surface.[147] Issues deserving of more attention include the mechanisms of solid state electrochemical behaviour and the electron storage properties which are rarely discussed. The advent of MOFs incorporating redox-active metals and linkers as well as higher electrical conductivities should also instigate further developments in MOFs for energy storage, and coupling of the electronic and ion motion should bring about higher gravimetric capacities.

3.6 Molecular electronics: sensors, switches and machines

An interesting possibility for redox-active MOFs is the prospect of exploiting the switchable nature of the redox states to bring about dynamic motion, as is relevant to molecular machines based on robust and dynamic bistable mechanically interlocked molecules. In this context, the NU-1000 framework incorporating trisradical rotaxanes has recently been addressed (Fig. 5).[148] In this proof-of-concept experiment, the MOF scaffold aided the organisation of rotaxanes, which incorporate redox-active viologen subunits that can be addressed electrochemically in the solid state. In particular, the electrochemical reduction resulted in electrochromic behaviour (blue to purple when the radical state is generated, as shown in Fig. 5). This ability to control the electrochromic properties of the material amongst others *via* a redox-active switch is appealing for the development of solid state molecular electronics devices such as molecular switches and machines.

The potential to alter the absorption and luminescence properties[93,94] of MOFs by exploiting the different characteristics of the redox states is a subject of great interest owing to their potential applications in optoelectronic devices, and as chemical sensors.[118,149] For example, a Mn(II) coordination solid based on the tris(4-(pyridin-4-yl)phenyl)amine ligand was found to exhibit switchable 'on'/'off' fluorescence (using chemical oxidation) based on the redox state of the ligand which can exist in its radical cation ('off') or neutral state ('on').[89] Both absorption and fluorescence switching were observed in a redox-switchable MOF that underwent a reversible single-crystal-to-single-crystal transformation.[150] In this case, the redox reaction involved the hydroquinone/quinone couple in a hydroxylated analogue of the well-known zirconium UiO-68 framework. The redox triggered transformation exploited a chemical reaction in

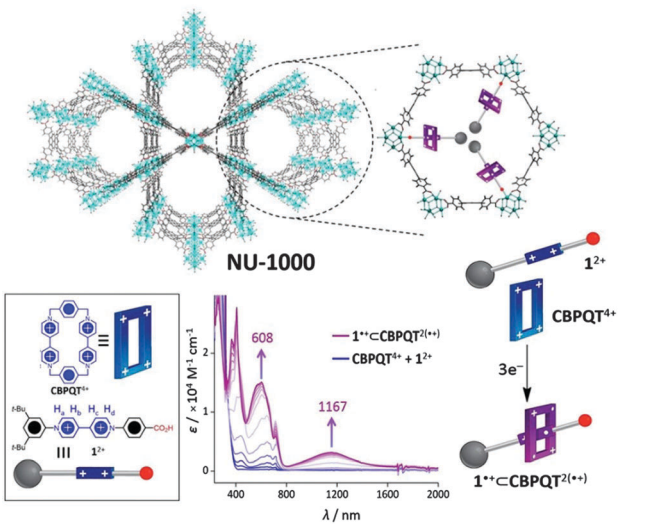

Fig. 5 Schematic of NU-1000 containing the semirotaxane (top). Representation of the semirotaxane components 1^{2+} and $CBPQT^{4+}$ (bottom left). Reduction of 1^{2+} and $CBPQT^{4+}$ with 3 mol e^- generates the semirotaxane $1^+\subset CBPQT^{2(+)}$ (bottom right and centre where the redox-dependent absorption spectrum is shown). Reproduced from ref. 148 with permission from National Academy of Sciences, USA.

the crystals, where iodobenzene diacetate was used as the oxidant and ascorbic acid as the reductant.

Different signal transduction methods have been considered for these redox-switchable MOFs, with electrical switching platforms being investigated for integration into devices.[118] MOFs exhibiting electrochemiluminescence properties are particularly attractive as their well-ordered porous structures result in high mass transfer capacities which support fast response times. Electrochemiluminescence is appealing due to the low background signal, high sensitivity and wide dynamic range for the detection of metal ions, small molecules and biomacromolecules. The first example involved a Zn^{II} framework which was prepared from a carboxylate modified $Ru(2,2'\text{-bpy})^{2+}$ moiety, where the Ru^{II} guest was electrochemically oxidised to Ru^{III}.[151] High electrochemiluminescence emission was observed due to facile electron transfer and was exploited to detect cocaine in serum relevant to illicit drug testing. Hybrid nanocomposites of MOFs with graphene oxide have also proven their utility for sensing acetaminophen and dopamine in serum and urine.[152]

Recently, the exploitation of redox activity in MOFs for a range of other electroanalytical applications such as nitrite detection has been demonstrated. Here, the development of new sensing devices are relevant to the food and health industries where the use of nitrite as a preserving agent requires close monitoring due to its potential toxicity in excess quantities. A thin film of MOF-525 was constructed from free-base porphyrin linkers and hexa-zirconium nodes on conducting substrates.[153] A remarkable current enhancement was detected in the presence of nitrite (NO_2^-) due to oxidation of NO_2^- to NO_2 by the porphyrin radical cation.

MOFs have also shown utility as alternatives to commercial enzymatic sensors which are currently used for electrochemical hydrogen peroxide (H_2O_2) and glucose sensing, areas of importance for clinical diagnostics (*e.g.* for diabetes management) and biotechnology.[118] In the presence of H_2O_2, the Co^{III} to Co^{II} reduction process in the framework $[Co(pbda)(bpy)\cdot 2H_2O]$ was sensitive to hydroxyl radicals with an associated colour change and fluorescence response.[154] $[Cu_3(btb)_2(H_2O)_3]$ (MOF-14) also demonstrated electrocatalytic activity towards H_2O_2 reduction and glucose oxidation.[155]

MOF biosensors have recently been developed for the detection of DNA *via* signal amplification processes. The PCN-222 framework incorporates a redox-active porphyrinic linker which was covalently bound with streptavidin.[156] A highly sensitive electrochemical DNA sensor was developed by integrating the electrocatalysis of porphyrinic MOF with a triple-helix molecular switch for signal transduction.[156] Hemin has also been encapsulated into Fe-MIL-88 (hemin@MOF) and applied as a redox probe for thrombin with the aid of an enzyme for signal amplification. Hemin is a well-known natural mellaoporphyrin with electroactivity owing to the Fe^{III}/Fe^{II} redox couple, but suffers as a catalyst from limited catalytic lifetime. Its incorporation into the host MOF matrix improved its stability, enabling the fabrication of devices from gold nanoparticles functionalised with hemin@MOF.[157]

3.7 Multifunctionality: the interplay between redox activity and magnetism

Magnetism in MOFs is a relatively well-studied genre.[158] The prospect of developing cooperative materials where the magnetic properties can be manipulated *via* redox state changes has attracted relatively limited attention.

The magnetic properties of Hoffman clathrate materials such as $[Fe(pyrazine)\{Pt(CN)_4\}]$ change markedly depending on the redox state of the Pt.[159] The iodine adduct $[Fe(pyrazine)\{Pt^{II/IV}(CN)_4(I)_n\}]$, prepared by oxidative addition of iodine to the open metal sites of Pt^{II}, raised the Curie temperature (T_c) by 100 K. Control of the iodine content (n = 0.0–1.0) resulted in systematic modulation of T_c in the range 300–400 K, showing that the spin transition temperature could be controlled between low and high spin states for magnetically bistable systems.

Systems involving synergistic magnetic and electronic properties are particularly interesting, especially cases where local spins and itinerant electrons interact.[160] For the conducting MOF $[(NBu_4)Fe_2^{III}(dhbq)_3]$, the reduced framework $[Na_{0.9}(NBu_4)_{1.8}Fe_2^{III}(dhbq)_3]$ exhibited significantly different conducting and magnetic properties.[63] In particular, the magnetic ordering temperature was found to increase in the reduced framework which was a relatively harder magnet due to the additional ligand radical spins which coupled antiferromagnetically to the Fe^{III} centres.

Frameworks based on mixed-valence $Ru^{II/III}$ paddlewheels bridged by polycyanide ligands such as TCNQ and its derivatives also exhibit a wide range of redox-dependent properties including antiferromagnetic coupling, long range ferromagnetic ordering and magnetism.[161–163]

These handful of examples, whilst limited in number, demonstrate the enormous future potential that exists for exploiting the different redox states of MOFs to tune magnetic properties of relevance to the development of new magnetoelectric devices for data storage applications, amongst others.[59,63]

4. Conclusions

Redox-active MOFs offer the prospect of accessing multiple tunable properties within a given material through manipulation of the redox state. Given the enormous recent strides in the area of conducting frameworks,[43,45] routes towards the implementation of these materials at the technological and industrial scales are on the horizon.[25,27] The majority of work in the area of redox-active MOFs to date has been focused on bulk synthesis and characterisation, however tremendous advances have been made recently in interfacing MOFs with surfaces, including conductive substrates.[20] These methods permit spatial control over the framework film architecture and thus the pore system, enabling the potential anisotropic properties of a framework to be exploited for directional charge transport.

At the fundamental level, the development of new computational methodologies to understand the mechanisms of charge transfer in MOFs is gaining momentum. Surface-anchored MOFs have already proven to be particularly relevant in this context.[102]

Clearly, there is a need for joint experimental, computational and theoretical approaches to explore redox activity. The highly ordered MOF scaffold provides unprecedented opportunities to explore deeply fundamental aspects of charge transfer in three-dimensional coordination space. These understandings promise to shed new light on aspects of charge migration in solar cells, for example, which lie at the heart of renewable clean energy technologies.[164]

Many significant challenges remain, however, and redox-active MOFs represent a fertile ground for chemists, physicists and engineers to unite their efforts. For the experimental chemist, the ongoing challenge lies in the often serendipitous nature of framework discovery. Nevertheless, principles of 'crystal engineering' are instructive in aiding the design of materials.[165] A particularly valuable pursuit in this regard is the development of isoreticular series of MOFs which enable systematic modulation of guest species in host MOFs. Ultimately, elucidating structure–function relationships will enable redox-active MOFs to be developed with desired practical functionality. Few systematic studies of this type exist at present; however, if the correct balance of redox-active components can be achieved (in terms of both their electronic and structural characteristics), potentially new fundamental charge transfer phenomena in MOFs may be realised. To date, results in this area suggest that historically important charge transfer theories such as classical and semiclassical theories for organic and inorganic mixed-valence complexes,[45] and CT theory for organic donor–acceptor salts,[59] may be useful for understanding charge transfer in coordination frameworks.

One caveat to note here is that defects are likely to play a crucial role in dictating the ensuing electronic properties. This issue has been discussed recently and methods are currently under development to control (and exploit) defects.[166,167] Significant efforts are required in this area, with combined experimental and computational approaches being a key strategy moving forwards.

Additional challenges and opportunities exist for the experimental chemist including understanding the electrochemistry of porous solids[18] and developing methods to modulate redox activity using external stimuli (light, pressure, electrical potential, *etc.*). While solid state spectroelectrochemical methods have proven to be valuable,[9,62] they are problematic when the porosities are low and redox processes are likely to be confined to the surface of MOF particles.

At the applied level, there is significant interest in the integration of redox-active materials into device architectures. Gaining real-time information about the properties of the different redox states (*e.g.*, their optical properties *via* spectroelectrochemical methods) is valuable here. In particular, it is important to ascertain the structural integrity of a material over repeat redox cycles, especially for practical applications.

Despite a number of crucial challenges for redox-active MOFs at both the fundamental and applied levels, their structural characteristics are highly advantageous. Coupled with new directions in achieving conductivity in these materials, enormous future potential exists to revolutionise a number of fields, particularly those relating to clean energy technologies (fuel cells, batteries, electrocatalysts and solar cells, amongst others).[144]

List of acronyms for ligands (alphabetical order)

aqdc	2,7-Anthraquinonedicarboxylate
bdc	1,4-Benzene dicarboxylate
bdc-NH_2	2-Aminobenzene-1,4-dicarboxylate
bht	Benzenehexathiol
bpdc	4,4′-Biphenyl dicarboxylate
bpy	4,4′-Bipyridine
2,2′-bpy	2,2′-Bipyridine
btb	1,3,5-Benzene tribenzoate
btc	1,3,5-Benzene tricarboxylate
$CBPQT^{4+}$	Cyclobis(paraquat-*p*-phenylene)
Cp*	Pentamethylcyclopentadienyl
DBMBI	*N*,*N*′-Di-(4-pyridylmethyl)-1,2,4,5-benzenetetracarboxydiimide
DCNQI	*N*,*N*′-Dicyanoquinonediimine
dcppy	2-Phenylpyridine-5,4′-dicarboxylate
$dhbq^{2-/3-}$	2,5-Dioxidobenzoquinone/1,2-dioxido-4,5-semiquinone
dobdc	2,5-Dioxido-1,4-benzenedicarboxylate
DPNI	*N*,*N*′-Di(4-pyridyl)-1,4,5,8-naphthalenetetracaboxydiimide
dsbdc	2,5-Dithiolatebenzene
Fc	Ferrocenyl
Fcdc	1,1′-Ferrocene dicarboxylate
hitp	2,3,6,7,10,11-Hexaiminotriphenylenesemiquinonate
H_4TBAPy	1,3,6,8-Tetrakis(*p*-benzoic acid)pyrene
ndc	2,6-Naphthalene dicarboxylate
	N,*N*′-Dicyanoquinodiimine
NDI	1,4,5,8-Napthalene tetracarboxydiimide
pbda	3-(Pyridine-3-yloxy)benzene-1,2-dicarboxylate
pdt	Pyrazine-2,3-dithiolate
TCNQ	7,7,8,8-Tetracyanoquinodimethane
tcpp	5,10,15,20-(4-Carboxyphenyl)porphyrin
TTF	Tetrathiafulvalene
TTFTB	Tetrathiafulvalene tetrabenzoate
TTFTC	Tetrathiafulvalene tetracarboxylate

Acknowledgements

The author gratefully acknowledges the support of a 2015 ChemComm Emerging Investigator Award and the Australian Research Council.

Notes and references

1 B. F. Hoskins and R. Robson, *J. Am. Chem. Soc.*, 1990, **112**, 1546–1554.
2 O. M. Yaghi, G. Li and H. Li, *Nature*, 1995, **378**, 703–706.

3 S. R. Batten, S. M. Neville and D. R. Turner, *Coordination Polymers: Design, Analysis and Application*, Royal Society of Chemistry, 2008.
4 S. Kitagawa and R. Matsuda, *Coord. Chem. Rev.*, 2007, **251**, 2490–2509.
5 A. A. Karyakin, *Electroanalysis*, 2001, **13**, 813–819.
6 D. Maspoch, D. Ruiz-Molina and J. Veciana, *Chem. Soc. Rev.*, 2007, **36**, 770–818.
7 B. Kong, C. Selomulya, G. F. Zheng and D. Y. Zhao, *Chem. Soc. Rev.*, 2015, **44**, 7997–8018.
8 M. B. Robin and P. Day, in *Adv. Inorg. Chem. Radiochem.*, ed. H. J. Emeléus and A. G. Sharpe, Academic Press, 1968, vol. 10, pp. 247–422.
9 P. M. Usov, C. Fabian and D. M. D'Alessandro, *Chem. Commun.*, 2012, **48**, 3945–3947.
10 A. Karmakar, A. V. Desai and S. K. Ghosh, *Coord. Chem. Rev.*, 2016, **307**, 313–341.
11 J. A. Johnson, X. Zhang, X. Zhang and J. Zhang, *Curr. Org. Chem.*, 2014, **18**, 1973–2001.
12 G. Givaja, P. Amo-Ochoa, C. J. Gomez-Garcia and F. Zamora, *Chem. Soc. Rev.*, 2012, **41**, 115–147.
13 A. Morozan and F. Jaouen, *Energy Environ. Sci.*, 2012, **5**, 9269–9290.
14 P. Ramaswamy, N. E. Wong and G. K. H. Shimizu, *Chem. Soc. Rev.*, 2014, **43**, 5913–5932.
15 S. Horike, D. Umeyama and S. Kitagawa, *Acc. Chem. Res.*, 2013, **46**, 2376–2384.
16 H. Al-Kutubi, J. Gascon, E. J. R. Sudholter and L. Rassaei, *ChemElectroChem*, 2015, **2**, 462–474.
17 M. Li and M. Dincă, *J. Am. Chem. Soc.*, 2011, **133**, 12926–12929.
18 J. E. Halls, D. Jiang, A. D. Burrows, M. A. Kulandainathan and F. Marken, *Electrochemistry*, 2014, **12**, 187–210.
19 N. Stock and S. Biswas, *Chem. Rev.*, 2012, **112**, 933–969.
20 P. Falcaro, R. Ricco, C. M. Doherty, K. Liang, A. J. Hill and M. J. Styles, *Chem. Soc. Rev.*, 2014, **43**, 5513–5560.
21 J. L. Zhuang, A. Terfort and C. Wöll, *Coord. Chem. Rev.*, 2016, **307**, 391–424.
22 O. Shekhah, J. Liu, R. A. Fischer and C. Wöll, *Chem. Soc. Rev.*, 2011, **40**, 1081–1106.
23 D. Zacher, O. Shekhah, C. Wöll and R. A. Fischer, *Chem. Soc. Rev.*, 2009, **38**, 1418–1429.
24 D. Bradshaw, A. Garai and J. Huo, *Chem. Soc. Rev.*, 2012, **41**, 2344–2381.
25 V. Stavila, A. A. Talin and M. D. Allendorf, *Chem. Soc. Rev.*, 2014, **43**, 5994–6010.
26 M. D. Allendorf, A. Schwartzberg, V. Stavila and A. A. Talin, *Chem. – Eur. J.*, 2011, **17**, 11372–11388.
27 M. D. Allendorf and V. Stavila, *CrystEngComm*, 2015, **17**, 229–246.
28 P. M. Usov, C. McDonnell-Worth, F. Zhou, D. R. MacFarlane and D. M. D'Alessandro, *Electrochim. Acta*, 2015, **153**, 433–438.
29 T. B. Faust and D. M. D'Alessandro, *RSC Adv.*, 2014, **4**, 17498–17512.
30 M. Meilikhov, K. Yusenko and R. A. Fischer, *Dalton Trans.*, 2010, **39**, 10990–10999.
31 J. E. Halls, S. D. Ahn, D. Jiang, L. L. Keenan, A. D. Burrows and F. Marken, *J. Electroanal. Chem.*, 2013, **689**, 168–175.
32 J. E. Halls, C. Y. Cummings, J. Ellis, L. L. Keenan, D. Jiang, A. D. Burrows and F. Marken, *Mol. Cryst. Liq. Cryst.*, 2012, **554**, 12–21.
33 C. K. Brozek and M. Dincă, *J. Am. Chem. Soc.*, 2013, **135**, 12886–12891.
34 C. K. Brozek, J. T. Miller, S. A. Stoian and M. Dincă, *J. Am. Chem. Soc.*, 2015, **137**, 7495–7501.
35 K. Hirai, H. Uehara, S. Kitagawa and S. Furukawa, *Dalton Trans.*, 2012, **41**, 3924–3927.
36 J. E. Halls, A. Hernan-Gomez, A. D. Burrows and F. Marken, *Dalton Trans.*, 2012, **41**, 1475–1480.
37 M. Meilikhov, K. Yusenko and R. A. Fischer, *J. Am. Chem. Soc.*, 2009, **131**, 9644–9645.
38 I. Hod, W. Bury, D. M. Gardner, P. Deria, V. Roznyatovskiy, M. R. Wasielewski, O. K. Farha, J. T. Hupp, W. Bury and O. K. Farha, *J. Phys. Chem. Lett.*, 2015, **6**, 586–591.
39 S. R. Ahrenholtz, C. C. Epley and A. J. Morris, *J. Am. Chem. Soc.*, 2014, **136**, 2464–2472.
40 I. Hod, W. Bury, D. M. Karlin, P. Deria, C.-W. Kung, M. J. Katz, M. So, B. Klahr, D. Jin, Y.-W. Chung, T. W. Odom, O. K. Farha and J. T. Hupp, *Adv. Mater.*, 2014, **26**, 6295–6300.
41 C. R. Wade, M. Li and M. Dincă, *Angew. Chem., Int. Ed.*, 2013, **52**, 13377–13381.
42 I. Hod, M. D. Sampson, P. Deria, C. P. Kubiak, O. K. Farha and J. T. Hupp, *ACS Catal.*, 2015, **5**, 6302–6309.
43 L. Sun, M. G. Campbell and M. Dincă, *Angew. Chem., Int. Ed.*, 2016, DOI: 10.1002/anie.201506219.
44 D. M. D'Alessandro, J. R. R. Kanga and J. S. Caddy, *Aust. J. Chem.*, 2011, **64**, 718–722.
45 M. D. Allendorf, M. E. Foster, F. Leonard, V. Stavila, P. L. Feng, F. P. Doty, K. Leong, E. Y. Ma, S. R. Johnston and A. A. Talin, *J. Phys. Chem. Lett.*, 2015, **6**, 1182–1195.
46 T. C. Narayan, T. Miyakai, S. Seki and M. Dincă, *J. Am. Chem. Soc.*, 2012, **134**, 12932–12935.
47 S. S. Park, E. R. Hontz, L. Sun, C. H. Hendon, A. Walsh, T. Van Voorhis and M. Dincă, *J. Am. Chem. Soc.*, 2015, **137**, 1774–1777.
48 A. Aumüller, P. Erk, G. Klebe, S. Hünig, J. U. von Schütz and H.-P. Werner, *Angew. Chem., Int. Ed.*, 1986, **25**, 740–741.
49 D. Sheberla, L. Sun, M. A. Blood-Forsythe, S. Er, C. R. Wade, C. K. Brozek, A. Aspuru-Guzik and M. Dincă, *J. Am. Chem. Soc.*, 2014, **136**, 8859–8862.
50 T. Kambe, R. Sakamoto, K. Hoshiko, K. Takada, M. Miyachi, J.-H. Ryu, S. Sasaki, J. Kim, K. Nakazato, M. Takata and H. Nishihara, *J. Am. Chem. Soc.*, 2013, **135**, 2462–2465.
51 G. Saito and Y. Yoshida, *Bull. Chem. Soc. Jpn.*, 2007, **80**, 1–137.
52 M. R. Bryce, *Chem. Soc. Rev.*, 1991, **20**, 355–390.
53 K. P. Goetz, D. Vermeulen, M. E. Payne, C. Kloc, L. E. McNeil and O. D. Jurchescu, *J. Mater. Chem. C*, 2014, **2**, 3065–3076.
54 J. Ferraris, D. O. Cowan, V. Walatka and J. H. Perlstein, *J. Am. Chem. Soc.*, 1973, **95**, 948–949.
55 J. B. Torrance, *Mol. Cryst. Liq. Cryst.*, 1985, **126**, 55–67.
56 J. Torrance, J. Vazquez, J. Mayerle and V. Lee, *Phys. Rev. Lett.*, 1981, **46**, 253.
57 G. Saito and T. Murata, *Philos. Trans. R. Soc., A*, 2008, **366**, 139–150.
58 S. Takaishi, M. Hosoda, T. Kajiwara, H. Miyasaka, M. Yamashita, Y. Nakanishi, Y. Kitagawa, K. Yamaguchi, A. Kobayashi and H. Kitagawa, *Inorg. Chem.*, 2009, **48**, 9048.
59 H. Miyasaka, *Acc. Chem. Res.*, 2013, **46**, 248–257.
60 K. J. Erickson, F. Leonard, V. Stavila, M. E. Foster, C. D. Spataru, R. E. Jones, B. M. Foley, P. E. Hopkins, M. D. Allendorf and A. A. Talin, *Adv. Mater.*, 2015, **27**, 3453–3459.
61 A. A. Talin, A. Centrone, A. C. Ford, M. E. Foster, V. Stavila, P. Haney, R. A. Kinney, V. Szalai, F. El Gabaly, H. P. Yoon, F. Leonard and M. D. Allendorf, *Science*, 2014, **343**, 66–69.
62 C. F. Leong, B. Chan, T. B. Faust and D. M. D'Alessandro, *Chem. Sci.*, 2014, **5**, 4724–4728.
63 L. E. Darago, M. L. Aubrey, C. J. Yu, M. I. Gonzalez and J. R. Long, *J. Am. Chem. Soc.*, 2015, **137**, 15703–15711.
64 G. Férey, F. Millange, M. Morcrette, C. Serre, M. L. Doublet, J. M. Greneche and J. M. Tarascon, *Angew. Chem., Int. Ed.*, 2007, **46**, 3259–3263.
65 H. J. Choi and M. P. Suh, *J. Am. Chem. Soc.*, 2004, **126**, 15844–15851.
66 G. C. Allen and N. S. Hush, *Prog. Inorg. Chem.*, John Wiley & Sons, Inc., 1967, pp. 357–389.
67 S. J. England, P. Kathirgamanathan and D. R. Rosseinsky, *J. Chem. Soc., Chem. Commun.*, 1980, 840–841.
68 P. H. Dinolfo, M. E. Williams, C. L. Stern and J. T. Hupp, *J. Am. Chem. Soc.*, 2004, **126**, 12989–13001.
69 A. Heckmann and C. Lambert, *Angew. Chem., Int. Ed.*, 2012, **51**, 326–392.
70 N. S. Hush, *Prog. Inorg. Chem.*, 1967, **8**, 391–444.
71 M. D. Ward, *Chem. Soc. Rev.*, 1995, **24**, 121–134.
72 D. M. D'Alessandro and F. R. Keene, *Chem. Soc. Rev.*, 2006, **35**, 424–440.
73 D. M. D'Alessandro and F. R. Keene, *Chem. Rev.*, 2006, **106**, 2270–2298.
74 K. D. Demadis, C. M. Hartshorn and T. J. Meyer, *Chem. Rev.*, 2001, **101**, 2655–2685.
75 J. N. Behera, D. M. D'Alessandro, N. Soheilnia and J. R. Long, *Chem. Mater.*, 2009, **21**, 1922–1926.
76 A. D. Carbó, *Electrochemistry of porous materials*, CRC press, 2009.
77 A. Domenech, H. Garcia, M. T. Domenech-Carbo and F. Llabres-I-Xamena, *J. Phys. Chem. C*, 2007, **111**, 13701–13711.
78 F. Scholz, L. Nitschke and G. Henrion, *Electroanalysis*, 1990, **2**, 85–87.

79 A. M. Bond and F. Scholz, *Langmuir*, 1991, **7**, 3197–3204.
80 A. F. Cozzolino, C. K. Brozek, R. D. Palmer, J. Yano, M. Li and M. Dincă, *J. Am. Chem. Soc.*, 2014, **136**, 3334–3337.
81 W. Kaim and J. Fiedler, *Chem. Soc. Rev.*, 2009, **38**, 3373–3382.
82 L. Dunsch, *J. Solid State Electrochem.*, 2011, **15**, 1631–1646.
83 F. J. Rizzuto, T. B. Faust, B. Chan, C. Hua, D. M. D'Alessandro and C. J. Kepert, *Chem. – Eur. J.*, 2014, **20**, 17597–17605.
84 S. Adeel, M. E. Abdelhamid, A. Nafady, Q. Li, L. L. Martin and A. M. Bond, *RSC Adv.*, 2015, **5**, 18384–18390.
85 S. M. Adeel, L. L. Martin and A. M. Bond, *J. Solid State Electrochem.*, 2014, **18**, 3287–3298.
86 S. V. Bhosale, C. H. Jani and S. J. Langford, *Chem. Soc. Rev.*, 2008, **37**, 331–342.
87 E. Coronado, M. Clemente-Leon, J. R. Galan-Mascaros, C. Gimenez-Saiz, C. J. Gomez-Garcia and E. Martinez-Ferrero, *J. Chem. Soc., Dalton Trans.*, 2000, 3955–3961.
88 G. Andric, J. F. Boas, A. M. Bond, G. D. Fallon, K. P. Ghiggino, C. F. Hogan, J. A. Hutchison, M. A. P. Lee, S. J. Langford, J. R. Pilbrow, G. J. Troup and C. P. Woodward, *Aust. J. Chem.*, 2004, **57**, 1011–1019.
89 C. Hua and D. M. D'Alessandro, *CrystEngComm*, 2014, **16**, 6331–6334.
90 C. Hua, P. Turner and D. M. D'Alessandro, *Dalton Trans.*, 2013, **42**, 6310–6313.
91 Y. J. Colon, D. Fairen-Jimenez, C. E. Wilmer and R. Q. Snurr, *J. Phys. Chem. C*, 2014, **118**, 5383–5389.
92 F.-X. Coudert and A. H. Fuchs, *Coord. Chem. Rev.*, 2016, **307**, 211–236.
93 S. Patwardhan and G. C. Schatz, *J. Phys. Chem. C*, 2015, **119**, 24238–24247.
94 S. Yin, L. Li, Y. Yang and J. R. Reimers, *J. Phys. Chem. C*, 2012, **116**, 14826–14836.
95 N. S. Hush, *J. Chem. Phys.*, 1958, **28**, 962–972.
96 R. A. Marcus, *Rev. Mod. Phys.*, 1993, **65**, 599–610.
97 R. A. Marcus, *J. Chem. Phys.*, 1956, **24**, 966–978.
98 D. M. Pajerowski, T. Watanabe, T. Yamamoto and Y. Einaga, *Phys. Rev. B: Condens. Matter Mater. Phys.*, 2011, **83**, 153202.
99 S. Grimme, *Chem. – Eur. J.*, 2012, **18**, 9955–9964.
100 R. B. Getman, Y.-S. Bae, C. E. Wilmer and R. Q. Snurr, *Chem. Rev.*, 2011, **112**, 703–723.
101 M. A. Addicoat, N. Vankova, I. F. Akter and T. Heine, *J. Chem. Theory Comput.*, 2014, **10**, 880–891.
102 J. Liu, W. Zhou, J. Liu, I. Howard, G. Kilibarda, S. Schlabach, D. Coupry, M. Addicoat, S. Yoneda, Y. Tsutsui, T. Sakurai, S. Seki, Z. Wang, P. Lindemann, E. Redel, T. Heine and C. Woell, *Angew. Chem., Int. Ed.*, 2015, **54**, 7441–7445.
103 B. Lukose, B. Supronowicz, P. S. Petkov, J. Frenzel, A. B. Kuc, G. Seifert, G. N. Vayssilov and T. Heine, *Condens. Matter*, 2011, 1–8.
104 C. H. Hendon, K. E. Wittering, T.-H. Chen, W. Kaveevivitchai, I. Popov, K. T. Butler, C. C. Wilson, D. L. Cruickshank, O. S. Miljanic and A. Walsh, *Nano Lett.*, 2015, **15**, 2149–2154.
105 A. Das and D. M. D'Alessandro, *CrystEngComm*, 2015, **17**, 706–718.
106 K. L. Mulfort and J. T. Hupp, *J. Am. Chem. Soc.*, 2007, **129**, 9604–9605.
107 C. F. Leong, T. B. Faust, P. Turner, P. M. Usov, C. J. Kepert, R. Babarao, A. W. Thornton and D. M. D'Alessandro, *Dalton Trans.*, 2013, **42**, 9831–9839.
108 Y.-S. Bae, B. G. Hauser, O. K. Farha, J. T. Hupp and R. Q. Snurr, *Microporous Mesoporous Mater.*, 2011, **141**, 231–235.
109 Y.-S. Bae, K. L. Mulfort, H. Frost, P. Ryan, S. Punnathanam, L. J. Broadbelt, J. T. Hupp and R. Q. Snurr, *Langmuir*, 2008, **24**, 8592–8598.
110 K. L. Mulfort, T. M. Wilson, M. R. Wasielewski and J. T. Hupp, *Langmuir*, 2009, **25**, 503–508.
111 M. Meilikhov, K. Yusenko, D. Esken, S. Turner, G. Van Tendeloo and R. A. Fischer, *Eur. J. Inorg. Chem.*, 2010, 3701–3714.
112 H. R. Moon, D. W. Lim and M. P. Suh, *Chem. Soc. Rev.*, 2013, **42**, 1807–1824.
113 C. Hua, A. Rawal, T. B. Faust, P. D. Southon, R. Babarao, J. M. Hook and D. M. D'Alessandro, *J. Mater. Chem. A*, 2014, **2**, 12466–12474.
114 D. M. D'Alessandro, B. Smit and J. R. Long, *Angew. Chem., Int. Ed.*, 2010, **49**, 6058–6082.
115 C. A. Grande and A. E. Rodrigues, *Int. J. Greenhouse Gas Control*, 2008, **2**, 194–202.
116 A. Subrenat, J. N. Baleo, P. Le Cloirec and P. E. Blanc, *Carbon*, 2001, **39**, 707–716.
117 R. J. Mortimer, in *Annu. Rev. Mater. Res.*, ed. D. R. Clarke and P. Fratzl, 2011, vol. 41, pp. 241–268.
118 L. E. Kreno, K. Leong, O. K. Farha, M. Allendorf, R. P. Van Duyne and J. T. Hupp, *Chem. Rev.*, 2012, **112**, 1105–1125.
119 H. H. Fei, S. Pullen, A. Wagner, S. Ott and S. M. Cohen, *Chem. Commun.*, 2015, **51**, 66–69.
120 C. W. Kung, T. C. Wang, J. E. Mondloch, D. Fairen-Jimenez, D. M. Gardner, W. Bury, J. M. Klingsporn, J. C. Barnes, R. Van Duyne, J. F. Stoddart, M. R. Wasielewski, O. K. Farha and J. T. Hupp, *Chem. Mater.*, 2013, **25**, 5012–5017.
121 L. Sun, T. Miyakai, S. Seki and M. Dincă, *J. Am. Chem. Soc.*, 2013, **135**, 8185–8188.
122 M. G. Campbell, D. Sheberla, S. F. Liu, T. M. Swager and M. Dincă, *Angew. Chem., Int. Ed.*, 2015, **54**, 4349–4352.
123 M. G. Campbell, S. F. Liu, T. M. Swager and M. Dincă, *J. Am. Chem. Soc.*, 2015, **137**, 13780–13783.
124 T. Kambe, R. Sakamoto, T. Kusamoto, T. Pal, N. Fukui, K. Hoshiko, T. Shimojima, Z. F. Wang, T. Hirahara, K. Ishizaka, S. Hasegawa, F. Liu and H. Nishihara, *J. Am. Chem. Soc.*, 2014, **136**, 14357–14360.
125 T. B. Faust, P. M. Usov, D. M. D'Alessandro and C. J. Kepert, *Chem. Commun.*, 2014, **50**, 12772–12774.
126 J. Cui and Z. Xu, *Chem. Commun.*, 2014, **50**, 3986–3988.
127 X.-Y. Li, Y.-G. Sun, P. Huo, M.-Y. Shao, S.-F. Ji, Q.-Y. Zhu and J. Dai, *Phys. Chem. Chem. Phys.*, 2013, **15**, 4016–4023.
128 Y. Kobayashi, B. Jacobs, M. D. Allendorf and J. R. Long, *Chem. Mater.*, 2010, **22**, 4120–4122.
129 B. Chen, Z.-P. Lv, C. F. Leong, Y. Zhao, D. M. D'Alessandro and J.-L. Zuo, *Cryst. Growth Des.*, 2015, **15**, 1861–1870.
130 B. S. Brunschwig, C. Creutz and N. Sutin, *Chem. Soc. Rev.*, 2002, **31**, 168–184.
131 X. Nie, A. Kulkarni and D. S. Sholl, *J. Phys. Chem. Lett.*, 2015, **6**, 1586–1591.
132 W. Xia, A. Mahmood, R. Q. Zou and Q. Xu, *Energy Environ. Sci.*, 2015, **8**, 1837–1866.
133 J. K. Sun and Q. Xu, *Energy Environ. Sci.*, 2014, **7**, 2071–2100.
134 Y. Q. Ren, G. H. Chia and Z. Q. Gao, *Nano Today*, 2013, **8**, 577–597.
135 S. L. Li and Q. Xu, *Energy Environ. Sci.*, 2013, **6**, 1656–1683.
136 S. Z. Li and F. W. Huo, *Nanoscale*, 2015, **7**, 7482–7501.
137 C.-W. Kung, T.-H. Chang, L.-Y. Chou, J. T. Hupp, O. K. Farha and K.-C. Ho, *Chem. Commun.*, 2015, **51**, 2414–2417.
138 S. B. Wang and X. C. Wang, *Small*, 2015, **11**, 3097–3112.
139 K. Meyer, M. Ranocchiari and J. A. van Bokhoven, *Energy Environ. Sci.*, 2015, **8**, 1923–1937.
140 T. Zhang and W. B. Lin, in *Metal–Organic Frameworks for Photonics Applications*, ed. B. Chen and G. Qian, 2014, vol. 157, pp. 89–104.
141 I. Hod, P. Deria, W. Bury, J. E. Mondloch, C.-W. Kung, M. So, M. D. Sampson, A. W. Peters, C. P. Kubiak, O. K. Farha and J. T. Hupp, *Nat. Commun.*, 2015, **6**, 8304.
142 Y. J. Han, J. F. Zhai, L. L. Zhang and S. J. Dong, *Nanoscale*, 2016, **8**, 1033–1039.
143 D. J. Xiao, E. D. Bloch, J. A. Mason, W. L. Queen, M. R. Hudson, N. Planas, J. Borycz, A. L. Dzubak, P. Verma, K. Lee, F. Bonino, V. Crocella, J. Yano, S. Bordiga, D. G. Truhlar, L. Gagliardi, C. M. Brown and J. R. Long, *Nat. Chem.*, 2014, **6**, 590–595.
144 L. Wang, Y. Z. Han, X. Feng, J. W. Zhou, P. F. Qi and B. Wang, *Coord. Chem. Rev.*, 2016, **307**, 361–381.
145 Z. Zhang, H. Yoshikawa and K. Awaga, *J. Am. Chem. Soc.*, 2014, **136**, 16112–16115.
146 K. M. Choi, H. M. Jeong, J. H. Park, Y. B. Zhang, J. K. Kang and O. M. Yaghi, *ACS Nano*, 2014, **8**, 7451–7457.
147 L. Wang, X. Feng, L. Ren, Q. Piao, J. Zhong, Y. Wang, H. Li, Y. Chen and B. Wang, *J. Am. Chem. Soc.*, 2015, **137**, 4920–4923.
148 P. R. McGonigal, P. Deria, I. Hod, P. Z. Moghadam, A.-J. Avestro, N. E. Horwitz, I. C. Gibbs-Hall, A. K. Blackburn, D. Chen, Y. Y. Botros, M. R. Wasielewski, R. Q. Snurr, J. T. Hupp, O. K. Farha and J. F. Stoddart, *Proc. Natl. Acad. Sci. U. S. A.*, 2015, **112**, 11161–11168.
149 X. J. Zhang, W. J. Wang, Z. J. Hu, G. N. Wang and K. S. Uvdal, *Coord. Chem. Rev.*, 2015, **284**, 206–235.
150 B. Gui, X. S. Meng, Y. Chen, J. W. Tian, G. L. Liu, C. C. Shen, M. Zeller, D. Q. Yuan and C. Wang, *Chem. Mater.*, 2015, **27**, 6426–6431.
151 Y. Xu, X. B. Yin, X. W. He and Y. K. Zhang, *Biosens. Bioelectron.*, 2015, **68**, 197–203.

152 X. Wang, Q. X. Wang, Q. H. Wang, F. Gao, F. Gao, Y. Z. Yang and H. X. Guo, *ACS Appl. Mater. Interfaces*, 2014, **6**, 11573–11580.
153 C.-W. Kung, T.-H. Chang, L.-Y. Chou, J. T. Hupp, O. K. Farha and K.-C. Ho, *Electrochem. Commun.*, 2015, **58**, 51–56.
154 L. Z. Yang, C. L. Xu, W. C. Ye and W. S. Liu, *Sens. Actuators, B*, 2015, **215**, 489–496.
155 D. Zhang, J. Zhang, R. Zhang, H. Shi, Y. Guo, X. Guo, S. Li and B. Yuan, *Talanta*, 2015, **144**, 1176–1181.
156 P. H. Ling, J. P. Lei and H. X. Ju, *Biosens. Bioelectron.*, 2015, **71**, 373–379.
157 S. B. Xie, J. W. Ye, Y. L. Yuan, Y. Q. Chai and R. Yuan, *Nanoscale*, 2015, **7**, 18232–18238.
158 E. Coronado and G. Minguez Espallargas, *Chem. Soc. Rev.*, 2013, **42**, 1525–1539.
159 R. Ohtani, K. Yoneda, S. Furukawa, N. Horike, S. Kitagawa, A. B. Gaspar, M. C. Munoz, J. A. Real and M. Ohba, *J. Am. Chem. Soc.*, 2011, **133**, 8600–8605.
160 B. Bechlars, D. M. D'Alessandro, D. M. Jenkins, A. T. Iavarone, S. D. Glover, C. P. Kubiak and J. R. Long, *Nat. Chem.*, 2010, **2**, 362–368.
161 X. Zhang, M. R. Saber, A. P. Prosvirin, J. H. Reibenspies, L. Sun, M. Ballesteros-Rivas, H. H. Zhao and K. R. Dunbar, *Inorg. Chem. Front.*, 2015, **2**, 904–911.
162 Z. Zhang, H. Zhao, M. M. Matsushita, K. Awaga and K. R. Dunbar, *J. Mater. Chem. C*, 2014, **2**, 399–404.
163 Z. Zhang, H. Zhao, H. Kojima, T. Mori and K. R. Dunbar, *Chem. – Eur. J.*, 2013, **19**, 3348–3357.
164 W. A. Maza, A. J. Haring, S. R. Ahrenholtz, C. C. Epley, S. Y. Lin and A. J. Morris, *Chem. Sci.*, 2016, **7**, 719–727.
165 R. Robson, *Dalton Trans.*, 2008, 5113–5131.
166 Z. Fang, B. Bueken, D. E. De Vos and R. A. Fischer, *Angew. Chem., Int. Ed.*, 2015, **54**, 7234–7254.
167 J. Canivet, M. Vandichel and D. Farrusseng, *Dalton Trans.*, 2016, **45**, 4090–4099.